XMAP from *Xenopus* Eggs Promotes Rapid Plus End Assembly of Microtubules and Rapid Microtubule Polymer Turnover

Robert J. Vasquez, David L. Gard,* and Lynne Cassimeris

Department of Molecular Biology, Lehigh University, Bethlehem, Pennsylvania 18015; and *Department of Biology, University of Utah, Salt Lake City, Utah 84112

Abstract. We have used video-enhanced DIC microscopy to examine the effects of XMAP, a M_r 215,000 microtubule-associated protein from *Xenopus* eggs (Gard, D. L., and M. W. Kirschner. 1987. *J. Cell Biol.* 105:2203–2215), on the dynamic instability of microtubules nucleated from axoneme fragments in vitro. Our results indicate that XMAP substantially alters the parameters of microtubule assembly at plus ends. Specifically, addition of 0.2 μM XMAP resulted in (*a*) 7–10-fold increase in elongation velocity, (*b*) approximately threefold increase in shortening velocity, and (*c*) near elimination of rescue (the switch from rapid shortening to elongation). Thus, addition of XMAP resulted in the assembly of longer, but more dynamic, microtubules from the plus ends of axonemes which upon catastrophe disassembled back to the axoneme nucleation site. In agreement with previous observations (Gard, D. L., and M. W. Kirschner. 1987. *J. Cell Biol.* 105:2203–2215), the effects of XMAP on the minus end were much less dramatic, with only a 1.5–3-fold increase in elongation velocity. These results indicate that XMAP, unlike brain MAPs, promotes both polymer assembly and turnover, and suggests that the interaction of XMAP with tubulin and the function of XMAP in vivo may differ from previously characterized MAPs.

MICROTUBULES (MTs)[1] are dynamic polymers which exhibit an unusual assembly process termed dynamic instability (Mitchison and Kirschner, 1984). Through this mechanism, MTs can exist in two distinct and persistent phases of elongation or rapid shortening, with abrupt and apparently random transitions between these phases (Mitchison and Kirschner, 1984; Walker et al., 1988). These transitions have been termed catastrophe (the transition from elongation to shortening) and rescue (the transition from shortening to elongation) (Walker et al., 1988). Since transitions occur randomly, MTs within a population behave asynchronously. At any given time, most MTs will be elongating while relatively few will be shortening rapidly (Mitchison and Kirschner, 1984; Walker et al., 1988). Because the lengths and lifetimes of individual MTs are dependent on dynamic instability, changes in the parameters of dynamic instability can have significant effects on the numbers and lengths of MTs in a population (Gliksman et al., 1993).

The molecular mechanism responsible for dynamic instability is unknown. However, current models suggest that a cap of tubulin-GTP subunits at the tip of the MT stabilizes the MT allowing continued addition of tubulin-GTP subunits to the polymer ends (Carlier et al., 1984; Mitchison and Kirschner, 1984). Hydrolysis of GTP results in a polymer composed primarily of tubulin-GDP. Loss of the tubulin-GTP cap, either by hydrolysis or tubulin-GTP dissociation, exposes the unstable core of tubulin-GDP subunits, resulting in a switch from elongation to rapid shortening (Hyman et al., 1992; for reviews see Erickson and O'Brien, 1992; Caplow, 1992). Conversely, recapping a shortening MT would result in a switch back to elongation (Mitchison and Kirschner, 1984; for reviews see Erickson and O'Brien, 1992; Caplow, 1992).

While MTs in living cells exhibit the phases of elongation and rapid shortening that are characteristic of dynamic instability, the rates and transition frequencies observed in vivo differ from those obtained with comparable concentrations of purified tubulin in vitro. Elongation typically is 5–10× faster and catastrophes and rescues are more frequent in cells compared to that observed with pure tubulin (Schulze and Kirschner, 1988; Sammak and Borisy, 1988; Cassimeris et al., 1988; Sheldon and Wadsworth, 1993; Tanaka and Kirschner, 1991). In addition, numerous variations on the basic theme of dynamic instability have been observed in different cell types and cytoplasmic extracts. For example, comparison of fibroblast and epithelial cell MTs has demonstrated that fibroblast MTs elongate faster, shorten faster, and rescue less frequently than epithelial cell MTs (Sheldon and

Please address all correspondence to Dr. Lynne Cassimeris, Department of Molecular Biology, 111 Research Drive, Lehigh University, Bethlehem, PA 18015. Telephone: (610) 758-6275; Fax: (610) 758-5851.

1. *Abbreviations used in this paper*: MAP, microtubule-associated protein; MT, microtubule; VE-DIC, video-enhanced differential interference light microscopy; XMAP, *Xenopus*, a 215-kD microtubule-associated protein.

© The Rockefeller University Press, 0021-9525/94/11/985/9 $2.00

Wadsworth, 1993). Clear differences in dynamic instability have been observed in cytoplasmic extracts switched between interphase and mitotic stages. In these extracts the switch from interphase to mitosis is accompanied by a small increase in elongation velocity and major changes in the transition frequencies (Belmont et al., 1990; Gliksman et al., 1992; Verde et al., 1992). Changes in these parameters, along with changes in the number of MTs, are sufficient to generate the MT lengths and turnover times characteristic of interphase or mitotic spindle MT arrays (Gliksman et al., 1993).

Based on the observations above, it has become clear that cells possess mechanisms to regulate dynamic instability and that this regulation plays a major role in determining MT organization and polymer turnover. Recent results suggest that microtubule-associated proteins (MAPs) play a major role in regulating dynamic instability. For example, addition of neuronal MAPs such as MAP2 or tau to pure tubulin in vitro promotes a modest increase in the rate of MT elongation (1–3-fold), while stabilizing MTs by reducing the frequency of catastrophe, promoting rescue, and reducing the rate of rapid shortening (Drechsel et al., 1992; Pryer et al., 1992; Kowalski and Williams, 1993). The overall stabilizing effect of these MAPs is consistent with their role in stabilizing axonal and dendritic MTs.

To gain more insight into the mechanisms by which MT assembly is regulated in nonneuronal cells, we have examined the effects of *Xenopus*, a 215-kD microtubule-associated protein (XMAP), a high molecular mass MAP isolated from *Xenopus* eggs, on MT assembly in vitro. XMAP (M_r 215,000) was originally identified and isolated based on its ability to promote the rapid assembly of MTs from centrosomes and axonemes in vitro (Gard and Kirschner, 1987*b*). By examining MT lengths in samples fixed at time points, XMAP was shown to specifically promote assembly of MT plus ends. In addition, XMAP was shown to be phosphorylated in a cell cycle–dependent manner (Gard and Kirschner, 1987*b*). For this report, we have used video-enhanced differential interference contrast light microscopy (VE-DIC) to examine the effects of XMAP on the dynamic instability of MTs in vitro. This assay provides a more accurate measurement of how XMAP affects the four parameters of dynamic instability. In agreement with published results (Gard and Kirschner, 1987*b*), we observed that XMAP exerts its effects largely on the plus end of MTs, with relatively little effect on the minus end. Our results indicate that while XMAP dramatically increases the rate of MT plus end elongation, it also promotes plus end MT turnover by increasing the rate of rapid shortening and decreasing rescue. Addition of XMAP thus results in a population of extremely long, but highly dynamic MTs. These results suggest that XMAP is functionally unique among the MAPs isolated to date. XMAP's unique effects on MT dynamics may play an important role in regulating the rapid assembly and reorganization of MTs during early *Xenopus* development.

Materials and Methods

Protein Purification

Tubulin was isolated from porcine brains by two cycles of assembly and disassembly and purified free of microtubule-associated proteins by phosphocellulose chromatography followed by a final assembly cycle in PEM buffer (0.1 M Pipes pH 6.9, 2 mM EGTA, 1 mM $MgSO_4$ and 0.5 mM GTP) supplemented with 1 M glutamate. This tubulin pellet was resuspended in PEM buffer, clarified, and stored at −75°C (Walker et al., 1988; Voter and Erickson, 1984). One tubulin preparation was used for all experiments. No MAPs were detected in this preparation by silver staining (Morrisey, 1981) of overloaded SDS-PAGE minigels (50 μg/lane; Walker et al., 1988). Tubulin concentration was determined as described by Drechsel et al. (1992). For video assays, small aliquots of tubulin were thawed, stored on ice, and used within 1–2 h.

Axoneme fragments were isolated from *S. purpuratus* sperm flagella as described by Bell et al. (1982) and Walker et al. (1988). Axonemes were stored at −20°C in 50% glycerol and washed in PEM buffer before use (Walker et al., 1988).

XMAP was isolated from *Xenopus* eggs as described previously (Gard and Kirschner, 1987*b*) with several modifications. First, eggs were not specifically activated before lysis; however, lysis should result in activation. Second, the following changes were made to the chromatography steps: XMAP was eluted from the phosphocellulose column with 150–300 mM NaCl; the salt gradient used to elute the mono Q column was 0–300 mM NaCl in 60 min; and Superose 6 FPLC was substituted for the TSK 400 column. Protein concentration was determined by scanning densitometry of Coomassie blue–stained gels using BSA as a standard. A typical yield from a liter of eggs was ~30–40 μg in <1 ml. Because freezing of XMAP causes a large loss in activity, the protein was shipped on ice from Utah to Pennsylvania. The protein was dialyzed for 1–2 h at 4°C against PEM containing 1 mM DTT and 1 μg/ml phenanthroline to remove the salt from the final chromatography elution. The protein was stored on ice and used within 2 d for all functional experiments. Quantitative data is presented from two XMAP preparations. Two additional preparations gave qualitatively similar results but were not included because sample size was limited or freezing of the protein occurred during shipping.

Microtubule Assembly Assays

The assembly of individual, axoneme-nucleated MTs was observed using VE-DIC (described below) by methods adapted from Walker et al. (1988). In preliminary experiments we found that XMAP bound to the glass surfaces of slide and coverslip. To minimize the adsorption of XMAP to glass we used the following protocol. Axoneme fragments were allowed to adhere to biologically clean coverslips (Lutz and Inoué, 1986) for 5 min in a humid chamber. MT assembly chambers were then constructed by placing the coverslips on top of clean glass slides using strips of parafilm for spacers. Top and bottom sides were sealed with VALAP (1:1:1 mixture of beeswax, lanolin, and petrolatum) to form a perfusion chamber with a volume of ~50 μl. Perfusion chambers were flushed with two volumes of PEM containing 0.5% NP-40 (PEM/NP-40) followed by perfusion and incubation with casein (5 mg/ml in distilled water) for 2 min (Block et al., 1990). Free casein was removed by flushing with two chamber volumes of PEM/NP-40. Pretreatment of the chambers in this manner had no noticeable effect on the dynamic instability of MTs assembled from purified tubulin.

MT assembly was initiated by introduction of tubulin (4–12 μM) in the absence or presence of XMAP. In addition to tubulin and XMAP, samples contained 1 mM GTP and 0.25 mg/ml casein in PEM/NP-40. Individual slides were warmed to 35°C on the microscope stage and were examined for 30–60 min. The concentrations of tubulin were kept low to minimize spontaneous assembly. In addition, the axoneme number concentration was kept low to ensure that the concentration of free tubulin remained constant over the course of an experiment. We estimate that at the tubulin and axoneme concentrations used here, <0.02% of tubulin dimers were incorporated into polymer. Finally, since axonemes nucleate the assembly of both plus and minus end MTs, kinetic measurements can be made at each end. The ends were distinguished based on the faster elongation rates of plus ends. Assembly of individual, axoneme-nucleated microtubules was visualized as described below.

Video Microscopy

Individual MTs were visualized using VE-DIC light microscopy (Schnapp, 1986; Salmon et al., 1989). We used a Nikon microphot-SA equipped with 60×/1.4 NA DIC Plan Apo lens, DIC prisms, and 1.4 NA condenser. Illumination was provided by a 100 W mercury lamp passed through an Ellis light scrambler (Technical Video, Woods Hole, MA). The microscope stand was also equipped with heat absorbing and 546-nm interference filters. Images were projected through a 5× projection lens to a 2400 newvicon video camera (Hamamatsu Corp., Bridgewater, NJ). Images were further en-

hanced using an Argus 10 (Hamamatsu Corp.) image processor for real-time, two frame exponential averaging. After passage through a time date generator (For-A Corp., Natick, MA) images were recorded onto super VHS video tapes using a Sony SV0-9500MD recorder. An Air Stream Stage Incubator (Nickolson Precision Instruments, Gaithersburg, MD) was used to heat the stage to 35°C. Stage temperature was monitored with a YSI telethermometer.

Micrographs were made by photographing the video monitor as described previously (Cassimeris et al., 1988).

Data Analysis

The rates of MT elongation and shortening were determined from video tapes using PC-based analysis software developed by Salmon and colleagues (Gliksman et al., 1992, Simon et al., 1992). For each MT, the change in MT length was plotted as a function of time and the average rate of elongation or shortening determined from least squares regression analysis. Plus and minus ends were assigned based on elongation velocities (Walker et al., 1988). Data is reported as the mean ± SEM. As noted previously by Drechsel et al. (1992), the error bars primarily reflect variations in rates between individual MTs. The actual error in measurement is small since repeated measurements of the elongation of individual MTs had standard deviations equal to ~5% of the mean.

The values for the association and dissociation rate constants during elongation were determined from plots of velocity vs tubulin concentration. Based on the following equation for elongation at each end:

$$v^e = k^e_{on}\,[\text{tubulin}] - k^e_{off} \quad (1)$$

where v^e is the elongation velocity. The association rate constant, k^e_{on}, is proportional to the slope and the dissociation rate constant, k^e_{off}, is proportional to the y-intercept (Walker et al., 1988).

The frequency of catastrophe at each tubulin concentration was determined by summing the total time spent in elongation for all MTs of a given polarity divided by the number of catastrophes observed (Walker et al., 1988). MTs assembled in the presence of XMAP at higher tubulin concentrations (10 μM) sometimes elongated out of the field of view. These MTs were considered in an elongation phase even though the end was not observed. The frequencies of rescue were determined by a similar method using the total time spent in rapid shortening divided by the number of rescues observed (Walker et al., 1988).

Dynamicity, a measure of tubulin subunit addition or subtraction per unit time (Toso et al., 1993), was calculated from the total length MTs elongated and shortened divided by the total time spent in both phases. For comparison, published values for mean elongation and shortening velocities and mean times spent in both phases were used to calculate mean lengths of elongation and shortening. Dynamicity was then calculated from the mean lengths and mean times for elongation and shortening.

Results

XMAP was partially purified from unactivated *Xenopus* eggs by sequential ion exchange and gel filtration chromatography (Fig. 1; Gard and Kirschner, 1987*b*; see Materials and Methods). From the Coomassie blue-stained gel, we estimate that the 215-kD XMAP protein represents 85–90% of the total protein in the fractions with peak assembly promoting activity. While other minor protein components in these fractions might contribute to the functional activity, promotion of MT assembly precisely coelutes with the 215-kD XMAP polypeptide (Gard and Kirschner, 1987*b*; Gard, D. L., unpublished observations).

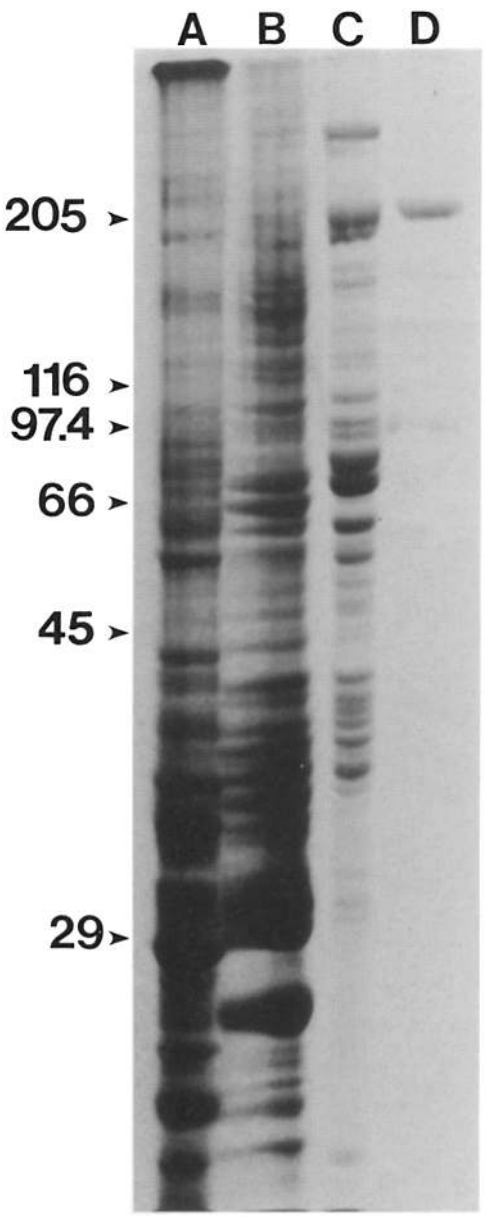

Figure 1. Coomassie blue-stained gel showing purification of XMAP from *Xenopus* eggs. (Lane *A*) total egg extract; (lane *B*) phosphocellulose 150 mM–300 mM fraction; (lane *C*) peak fractions from mono-Q chromatography; (lane *D*) peak fractions from Superose 6 chromatography. The XMAP band splits into a doublet when overloaded, as in lane *C*. Lane *D* shows the material used for functional studies.

XMAP Increases the Rates of Elongation and Shortening at MT Plus Ends

VE-DIC microscopy was used to follow the assembly of individual MTs in real time. Though the physiological temperature of *Xenopus laevis* is ~20°C, assembly reactions were carried out at 35°C to allow comparison with previously published results for pure tubulin and tubulin plus neuronal MAPs. MTs assembled from tubulin alone exhibited the characteristic behavior expected of dynamic instability. The measured rates of elongation, rapid shortening, catastrophe, and rescue were similar to those reported by Walker et al. (1988) indicating that buffer conditions and the preblocking protocol did not significantly alter assembly parameters.

In the presence of 0.2 μM XMAP, MTs underwent the characteristic phases and transitions of dynamic instability, but XMAP dramatically affected elongation and rapid shortening velocities at MT plus ends (Figs. 2 and 3). Addition of 0.2 μM XMAP to 4–10 μM tubulin increased the elongation velocity 7–10-fold over that seen with tubulin alone (Figs. 2, 3, and 4 *a*). In addition, the velocity of rapid shortening also was increased by XMAP. Since the velocity of

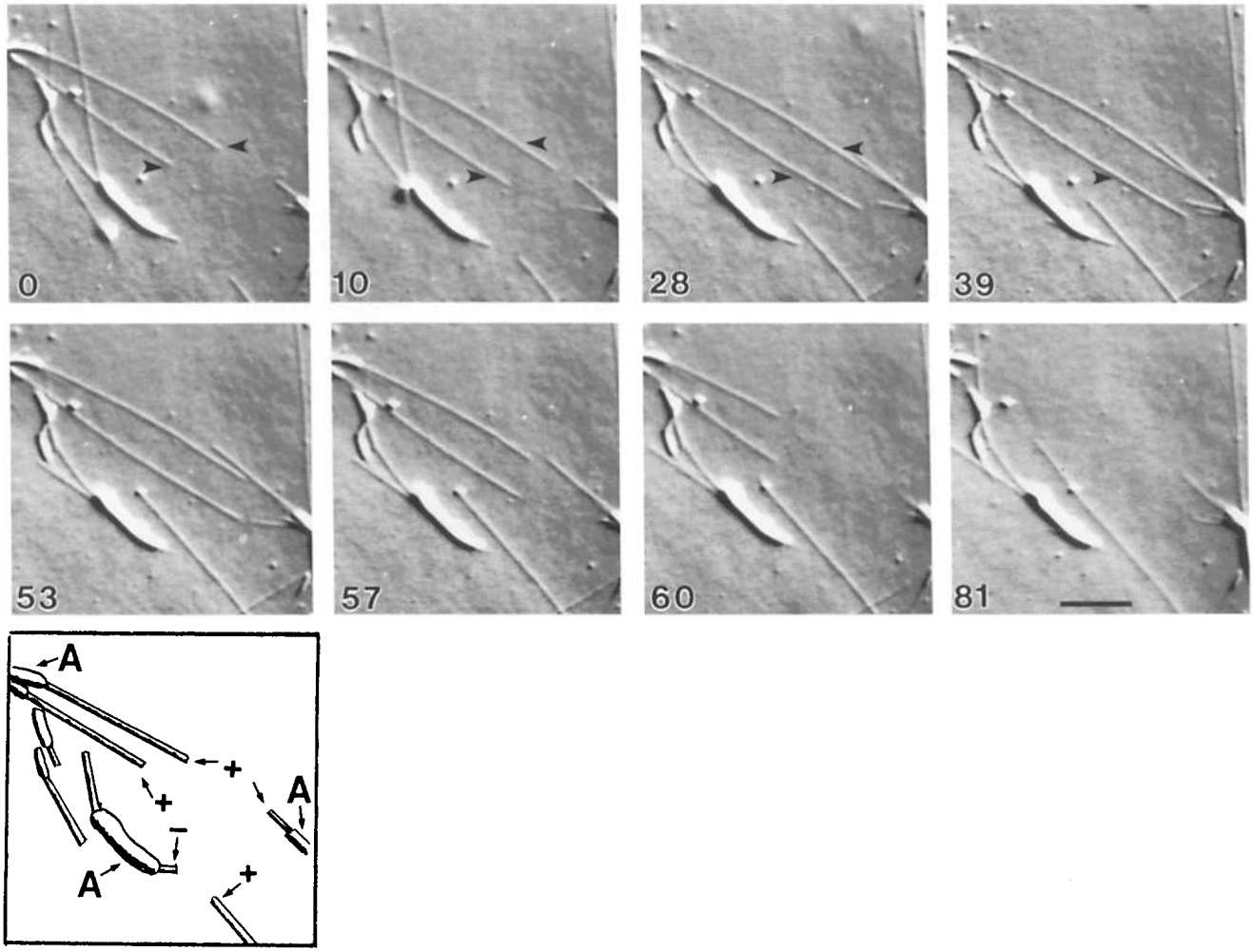

Figure 2. VE-DIC micrographs, taken from a real-time video recording, of axoneme-nucleated microtubules undergoing dynamic instability. MTs were assembled from 10 μM tubulin in the presence of 0.2 μM XMAP. Arrowheads mark the position of two plus ends in the first frame. The rapid assembly and shortening of these two plus ends are shown. Time, in seconds, is given in each frame. Bar, 5 μm. The sketch shows the position of several axonemes (*A*) and identifies the polarity of many MTs in the field.

rapid shortening was independent of tubulin concentration with or without XMAP (Walker et al., 1988; unpublished observations), we pooled plus end rapid shortening data from all tubulin concentrations examined and the results are shown in Fig. 4 *b*. Addition of XMAP increased the velocity of rapid shortening approximately threefold, from 18.8 ± 1.3 μm/min (SEM; n = 48) for MTs assembled from tubulin alone, to 49.9 ± 1.3 μm/min (SEM, n = 232) in the presence of XMAP (Figs. 3, 4, and Table I).

In contrast to the dramatic effects on elongation and rapid shortening velocities at plus ends, XMAP had comparatively small effects on the dynamic instability of MT minus ends

Table I. Rate Constants for Tubulin Association and Dissociation

	Plus ends		Minus ends	
	Tubulin	Tubulin + XMAP	Tubulin	Tubulin + XMAP
Slope (μm/μM min)	0.153	0.887	0.07	ND
k_{on}^{e} ($\mu M^{-1}s^{-1}$)	4.2	24	1.9	ND
x-intercept (μM)	3.5	0*	3.8	ND
y-intercept (μm/min)	−0.53	0*	−0.27	ND
k_{off}^{e} (s^{-1})	−15	0*	−7.4	ND
k_{off}^{rs} (s^{-1})	−512	−1359	−605	−641

Data are derived from plots shown in Fig. 4 (*a*) and (*b*) for plus ends and Fig. 5 (*a*) and (*b*) for minus ends. k_{on}^{e} is the association rate constant during elongation, k_{off}^{e} is the dissociation rate constant during elongation, and k_{off}^{rs} is the dissociation rate constant during shortening. Rate constants were calculated based on 1634 tubulin dimers/μm.

* For plus ends assembled with XMAP, the y-intercept was constrained through the origin as described in the text. This assumption sets k_{off}^{e} to zero.
ND, not determined.

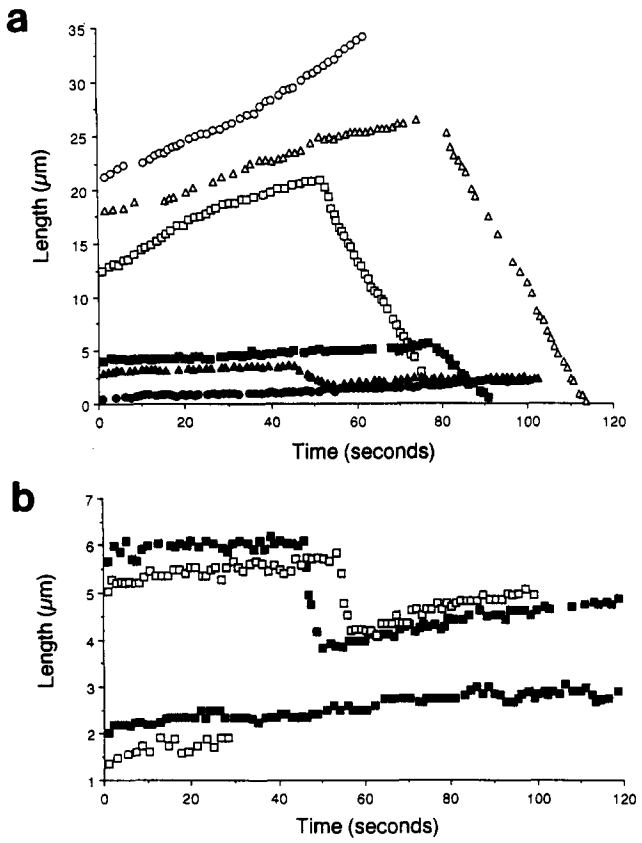

Figure 3. Plus (*a*) and minus (*b*) end life history plots of MTs assembled from 10 μM tubulin in the absence (*closed symbols*) and presence of 0.2 μM XMAP (*open symbols*). The lengths of individual MTs were measured from real time video tape recordings as described in Materials and Methods.

(Fig. 3). For example, addition of 0.2 μM XMAP to 10 μM tubulin increased elongation velocity from 0.37 μm/min (±0.03 SEM, n = 27) to 0.6 μm/min (±0.09 SEM, n = 20). XMAP did not affect minus end rapid shortening velocity (Fig. 5 *b*). We measured rates of minus end shortening of 22.2 ± 3.1 μm/min (SEM; n = 28) for MTs assembled from tubulin alone and 23.5 ± 2.7 μm/min (SEM; n = 29) for tubulin plus XMAP.

The great majority of MTs assembled with or without XMAP exhibited elongation and rapid shortening at nearly constant velocities (Fig. 3). As noted previously by Gildersleeve et al. (1992), individual MTs occasionally showed variations in elongation rates and these variations were observed in samples with or without XMAP. In addition, many MTs assembled in the presence of XMAP were observed to elongate or shorten apparently attached to the glass surface (Fig. 2). While this may represent residual adsorption of XMAP to the glass coverslip surface, MTs were also observed to elongate and shorten off the coverslip surface and these MTs showed the same behavior as those apparently attached to the glass surface (not shown). MTs assembled from pure tubulin were never observed adsorbed to glass.

XMAP Increases Plus End Elongation by an Increase in the Association Rate Constant

We measured plus end elongation velocities at a constant concentration of XMAP (0.2 μM) and a range of tubulin concentrations from 4 to 10 μM (Fig. 4 *a*). Few MTs were observed at 3 μM, limiting observations to tubulin concentrations ≥4 μM. Although the ratio of XMAP to tubulin was not held constant, elongation velocity still increased with increasing tubulin concentration. Because the ratio of XMAP to tubulin decreased at higher tubulin concentrations, it was necessary to constrain the linear regression analysis through the origin (to keep $k_{off} \leq 0$; Eq. 1). Constraint of the data through the origin assumes that the off rate constant is zero in the presence of XMAP. Given this assumption, addition of XMAP caused an apparent sixfold increase in the association rate constant from 4.2 $\mu M^{-1}s^{-1}$ for pure tubulin to 24 $\mu M^{-1}s^{-1}$ for tubulin assembled with XMAP (Table I).

As shown in Fig. 5 *a*, 0.2 μM XMAP increased minus end elongation velocity by ~1.5–3-fold over a range of tubulin

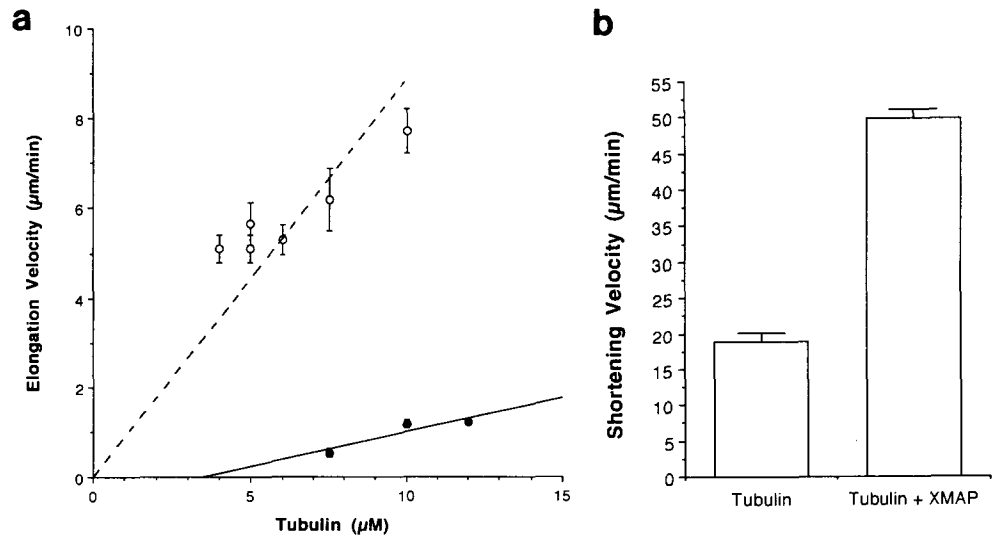

Figure 4. Parameters of dynamic instability for MT plus ends measured as a function of tubulin concentration. (*a*) Elongation velocities vs tubulin concentration, determined from life history plots of individual MTs. Data are plotted as mean ± SEM and for each concentration n ranged from 8–36 (tubulin alone) and 20–81 (plus XMAP). The error bars for tubulin samples are about the size of the graph symbol. Linear regression lines used to calculate rate constants are shown. The regression line through the XMAP data was constrained through the origin as described in the text. (*b*) Rapid shortening velocities in the absence and presence of 0.2 μM XMAP. Since rapid shortening was independent of tubulin concentration, data from all tubulin concentrations analyzed were averaged. Data is plotted as mean ± SEM, n = 51 for tubulin and 232 for tubulin plus XMAP.

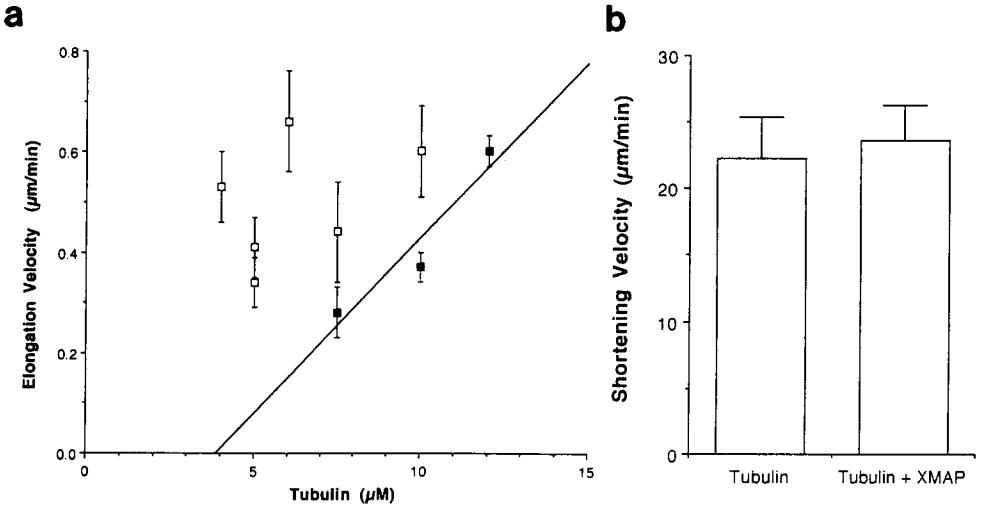

Figure 5. Parameters of dynamic instability at MT minus ends in the absence and presence of XMAP. (*a*) Elongation velocities vs tubulin concentration. Data are plotted as mean ± SEM, for each concentration *n* was 11–38 (tubulin) and 9–22 (plus XMAP). The linear regression line through the data for tubulin was used to calculate the rate constants. Rate constants were not determined for samples containing XMAP. (*b*) Rapid shortening velocities in the presence and absence of XMAP. Since rapid shortening velocity is independent of tubulin concentration, data are pooled from all tubulin concentrations analyzed and plotted as the mean ± SEM (n = 28 for tubulin and 29 for samples containing XMAP).

concentrations. The large scatter for the samples containing XMAP is likely a reflection of the small sample size, particularly at low tubulin concentrations. Therefore, rate constants were not calculated for minus ends assembled with XMAP.

Plus End Transition Frequencies: Catastrophes Are Not Altered but Rescues Are Infrequent in the Presence of XMAP

XMAP did not inhibit the transition of MT plus ends from elongation to rapid shortening (catastrophe). For example, at 7.5–10 μM tubulin, plus end catastrophes were observed about once every 57 s in the presence of XMAP (64 catastrophes during 3,646 s elongation) and once every 104 s in the absence of XMAP (26 catastrophes during 2,705 s elongation).

Although XMAP did not suppress catastrophe frequency, XMAP significantly reduced plus end rescue frequency. For pure tubulin at 7.5–10 μM, we observed plus end rescues once every 20 s of shortening (10 rescues during 200 s of shortening). At these same tubulin concentrations, we observed one rescue in 3,005 s of shortening for MTs assembled with XMAP. For all plus end MTs assembled with XMAP, we observed 232 MTs shorten for a total of ~43 min and only one of these underwent a rescue.

XMAP had little or no effect on transition frequencies at minus ends. For example, at 7.5–10 μM tubulin, minus ends underwent catastrophes about once every 156 s with XMAP (11 catastrophes during 1,715 s elongation) and once every 333 s without XMAP (17 catastrophes during 5,658 s elongation). In contrast to plus ends, rescues were observed frequently at minus ends assembled in the presence of XMAP. Minus end rescues, at 7.5–10 μM tubulin, were observed once every 19 s with XMAP (5 rescues for 95 s shortening) and once every 18 s without XMAP (8 rescues for 146 s shortening). Thus, XMAP did not appear to alter the minus end rescue frequency compared to that observed for pure tubulin.

Discussion

VE-DIC microscopic observations of individual MTs revealed that XMAP, a 215-kD protein from *Xenopus* eggs, has pronounced effects on the dynamic instability of MT plus ends. Addition of 0.2 μM XMAP promotes a 7–10-fold increase in elongation velocity, an approximately threefold increase in rapid shortening velocity and near complete suppression of rescue. The observed effect of XMAP on elongation velocity is strikingly similar to the overall effect of XMAP on MT plus end assembly reported by Gard and Kirschner (1987*b*), who used populations of MTs grown in solution and subsequently sedimented onto coverslips for immunofluorescence microscopy. The similar results obtained by these two studies suggest that possible adsorption of XMAP to the coverslips and slides in our assay has not significantly reduced its activity. It is unlikely that we have attained saturating concentrations of XMAP, and thus the magnitude of XMAP's effects may be increased further under saturating conditions.

XMAP Is Functionally Distinct from MAP2 and tau

Among the MAPs studied to date, XMAP has the unique property of specifically promoting assembly and disassembly of MT plus ends. The ability of XMAP to differentiate between plus and minus ends, and its effects on plus end dynamic instability, suggest that XMAP must interact with MTs differently than MAP2 and tau. These latter MAPs cause little or moderate increases in elongation velocity, decrease catastrophe frequency, increase rescue frequency, and slow shortening velocity at both MT ends (Pryer et al., 1992; Drechsel et al., 1992; Kowalski and Williams, 1993). Based on the novel end-specificity exhibited by XMAP, and the

Table II. Comparison of MT Dynamicity with XMAP or MAP2*

	Plus ends			Minus ends		
	Tb	Tb + MAP	Tb + MAP / Tb	Tb	Tb + MAP	Tb + MAP / Tb
XMAP‡	53.2	365	6.9	21.8	37.2	1.7
MAP2						
Pryer et al.,§ 1992	156	63.7	0.4	34.2	27.7	0.8
Kowalski and Williams,‖ 1993	54.5	30.9	0.6	ND	ND	ND

Published values for mean elongation and shortening velocities and frequencies of catastrophe and rescue were used to calculate MAP2 dynamicity.
* Calculated as described in Materials and Methods, all values in tubulin dimers/s.
‡ XMAP data pooled for 7.5 and 10 μM tubulin with and without 0.2 μM XMAP. Dynamicity values for 7.5 and 10 μM tubulin were pooled since the values at each concentration were similar.
§ Calculated at 10 μM tubulin with and without 1.25 μM MAP2.
‖ Calculated at 5 μM tubulin with and without 0.5 μM MAP2.
ND, not determined.

unique effects XMAP has on plus-end elongation velocity, shortening velocity, and rescue frequency, we predict that XMAP does not contain the MT-binding motif shared by tau, MAP2 and MAP4 (Chapin and Bulinski, 1992). Furthermore, the XMAP MT-binding site must be able to recognize the polarity inherent in the MT lattice. This does not seem unreasonable since it is likely that the motor proteins kinesin and dynein also show polarity-dependent MT binding.

In contrast to the differences noted above, XMAP shares with the mammalian brain MAPs the ability to promote MT assembly at low concentrations of tubulin where little or no assembly would be observed from pure tubulin (Figs. 4 *a* and 5 *a*). This promotion of assembly at low tubulin concentrations has been regarded previously as stabilization. In this sense, XMAP stabilizes MTs by lowering the critical concentration for elongation. However, in contrast to the neuronal MAPs, XMAP also stimulates polymer turnover. Polymer turnover can be measured by "dynamicity," a term introduced by Toso et al. (1993) to describe total tubulin dimer exchange per unit time. When we calculate dynamicity we find that XMAP increases dynamicity about sevenfold at plus ends and about twofold at minus ends (at 7.5–10 μM tubulin). In contrast, published data for MAP2 (Pryer et al., 1992; Kowalski and Williams, 1993) shows an approximate twofold reduction in dynamicity (Table II).

XMAP Increases the Plus End Association Rate Constant during Elongation

The 7–10-fold increase in elongation velocity observed with XMAP must result from an apparent increase in the association rate constant. Based on Eq. 1 and the rate constants for pure tubulin given in Table I, reducing the dissociation of tubulin subunits during elongation can only maximally increase elongation velocity by ≤2 fold. Thus, an increase in the association rate constant is required to generate the elongation velocities observed with XMAP, and our data suggest an apparent sixfold increase in the association rate constant (Fig. 4 *a*, Table I). This apparent increase in association rate constant is somewhat surprising, since assembly of pure tubulin has an association rate constant in the range of diffusion-limited reactions (Northrup and Erickson, 1992). Previous studies with tau also have suggested an increase in association rate constant (Drechsel et al., 1992). Several mechanisms can be proposed to increase a diffusion-limited rate of assembly.

First, XMAP may increase the number of sites for subunit addition. Since an MT is composed of 13 protofilaments, 1–13 elongating sites could exist at each end and increasing the number of protofilaments elongating could increase the apparent rate constant by approximately an order of magnitude. In this case each site would still elongate at a diffusion-limited rate. Second, XMAP could deliver oligomers to the plus ends of the polymer, and this could increase a rate constant apparently above a diffusion-limited maximum.

XMAP Increases Shortening Velocity at Plus Ends

The mechanism by which XMAP increases the rate of shortening is unknown. Rapid shortening is independent of tubulin concentration, both with and without XMAP, and is thought to reflect the first order dissociation of tubulin-GDP subunits from the MT lattice. The faster shortening velocity observed in the presence of XMAP was surprising since, as mentioned above, previously characterized neuronal MAPs slowed shortening. Mandelkow et al. (1991) have suggested that MT disassembly involves splaying apart of the protofilaments (Mandelkow et al., 1991) and this may reflect an initial weakening of lateral bonds between protofilaments before subsequent dissociation of subunits. XMAP may act to weaken interactions between protofilaments and thus increase the rate of protofilament splaying. Alternatively, XMAP may alter the tubulin conformation such that intersubunit associations are weakened.

Several other conditions have been identified which increase the velocity of rapid shortening. For pure tubulin, raising the magnesium concentration from 0.25 to 6 mM results in a 3–5-fold increase in shortening velocity at both plus and minus ends (O'Brien et al., 1990). Since XMAP only increases shortening velocity at plus ends, it is unlikely that XMAP increases shortening velocity by a similar mechanism. Recently we reported that enzymatic cleavage of the COOH terminus of β tubulin results in an approximately threefold increase in shortening velocity specifically at plus ends (Cassimeris, L. 1993. *Mol. Biol. Cell.* 4:165a). Since both XMAP and cleavage of β tubulin COOH terminus result in faster shortening only at MT plus ends, it is possible that XMAP interacts with this COOH-terminal region of β tubulin. However, based on XMAP's novel effects on MT assem-

bly, the interaction of XMAP with the COOH terminus of β tubulin must differ from those of tau, MAP2 and MAP4, which also bind to this same region (Serrano et al., 1984).

Plus End Transition Frequencies

Plus end catastrophes were not inhibited by XMAP even though XMAP causes a large increase in elongation velocity. At the fast elongation rates observed with XMAP, combined with the apparent lack of tubulin-GTP dissociation during elongation, build-up of an extensive GTP cap at plus ends and infrequent catastrophes would be expected, unless nucleotide hydrolysis remains coupled to subunit addition, as suggested previously for pure tubulin (Walker et al., 1988; Stewart et al., 1990; Bayley et al., 1990; O'Brien et al., 1987). Alternatively, MTs assembled with XMAP may have an altered conformation which results in frequent catastrophes.

Plus ends undergo infrequent rescues in the presence of XMAP. This may be related to the faster shortening velocity. If MTs assembled in the presence of XMAP have a less stable conformation, then it may be more difficult to recap the shortening polymer.

Possible Functions of XMAP in Xenopus Eggs and Early Embryos

The unique dynamic properties of MTs assembled in the presence of XMAP may play important roles in the regulation of MT assembly during oogenesis and early development in *Xenopus laevis*. Oogenesis requires significant reorganization of the oocyte MTs, including disassembly of the extensive prophase MT array and assembly of a unique MTOC and transient MT array (MTOC-TMA) (Gard, 1992). Additionally, fertilization of *Xenopus* eggs is accompanied by the assembly of a dramatic MT aster from the sperm centrosome. Within 30 min of fertilization, MTs from the sperm aster fill the egg cytoplasm (a diameter of 1.2 mm) (Stewart-Savage and Grey, 1982; Houlistan and Elinson, 1991; Schroeder and Gard, 1992). MTs extending from the sperm aster also form an extensive network in the vegetal cortex, where they play a major role in the rotation of the egg cortex that specifies the future dorsal-ventral axis of the developing embryo (Elinson and Rowning, 1988). Previous studies have suggested that assembly of the sperm aster would require MT assembly at rates of 30–50 μm/min (Gard and Kirschner, 1987*a*). Rates approaching this level (10–25 μm/min) have been measured in extracts of *Xenopus* eggs in vitro (Belmont et al., 1990; Verde et al., 1992; Parsons, S., and E. D. Salmon, personal communication). The promotion of MT assembly by XMAP observed here, if extrapolated to the tubulin concentration found in eggs ($\sim$25 μM; Gard and Kirschner, 1987*a*), would accelerate assembly to $\sim$25 μm/min. Thus XMAP is sufficient to account for the rapid rates required for assembly of the sperm aster and cortical MTs.

The rapid turnover of MTs promoted by XMAP also could play important roles in early development. The acceleration of MT shortening, in conjunction with mitotically activated severing factors (Vale, 1991; McNally and Vale, 1993; Shiina et al., 1992*a*), may speed MT disassembly during oocyte maturation and early cleavage. In particular, the extensive network of cortical MTs present during the first cell cycle after fertilization is rapidly disassembled shortly before cleavage (Schroeder and Gard, 1992). It should be noted that the velocity of shortening has not been measured in *Xenopus* eggs, but in cytoplasmic extracts, shortening velocities of only $\sim$10 μm/min have been observed (Belmont et al., 1990; Verde et al., 1992). This slower shortening velocity may reflect additional contributions from other MAPs, such as a recently described *Xenopus* egg 220–230 kD MAP (Shiina et al., 1992*b*; Faruki and Karsenti, 1994; Andersen, S. S. L., B. Buendia, J. E. Dominguez, and E. Karsenti. 1993. *Mol. Biol. Cell.* 4:266a). Regulation of MAP binding may allow subsets of egg MTs to shorten rapidly or to shorten without rescue. MTs in moitic sea urchin egg extracts exhibit shortening without rescue (Gliksman et al., 1992) and this may result from an XMAP-like protein and/or mitotic inactivation of rescue-promoting MAPs.

We are indebted to Ted Salmon, Neal Gliksman, and Steve Majors for their generous gift of the software program used for measuring MT lengths. Thanks to Ted Salmon, Nancy Pryer, and Richard Walker for many helpful discussions, and to K. Ferry, C. Spittle, N. Pryer, and D. Odde for critically reading the manuscript. L. Cassimeris and R. Vasquez are grateful to Guy Scala for help with microscopy.

Supported by grants from National Institutes of Health (L. Cassimeris) and National Science Foundation (D. L. Gard).

Received for publication 11 May 1994 and in revised form 10 August 1994.

References

Bayley, P. M., M. J. Schlistra, and S. R. Martin. 1990. Microtubule dynamic instability: numerical stimulation of microtubule transition properties using a lateral cap model. *J. Cell Sci.* 95:33–48.

Bell, C. W., C. Fraser, W. S. Sale, W.-J. Y. Tang, and I. R. Gibbons. 1982. Preparation and purification of dynein. *Methods Cell Biol.* 24:373–397.

Belmont, L. D., A. A. Hyman, K. E. Sawin, and T. J. Mitchison. 1990. Real time visualization of cell cycle dependent changes in microtubule dynamics in cytoplasmic extracts. *Cell.* 62:579–589.

Block, S. M., L. S. B. Goldstein, and B. J. Schnapp. 1990. Bead movement by single kinesin molecules studied with optical tweezers. *Nature (Lond.).* 348:348–352.

Caplow, M. 1992. Microtubule dynamics. *Curr. Opin. Cell Biol.* 4:58–65.

Carlier, M., T. L. Hill, and Y. Chen. 1984. Interference of GTP hydrolysis in the mechanism of microtubule assembly: an experimental study. *Proc. Natl. Acad. Sci. USA.* 81:771–775.

Cassimeris, L., N. K. Pryer, and E. D. Salmon. 1988. Real-time observations of microtubule dynamic instability in living cells. *J. Cell Biol.* 107:2223–2231.

Chapin, S. J., and J. C. Bulinski. 1992. Microtubule stabilization by assembly-promoting microtubule-associated proteins: a repeat performance. *Cell Motil. Cytoskeleton.* 23:236–243.

Drechsel, D. N., A. A. Hyman, M. H. Cobb, and M. W. Kirschner. 1992. Modulation of the dynamic instability of tubulin assembly by the microtubule-associated protein tau. *Mol. Biol. Cell.* 3:1141–1154.

Elinson, R., and B. Rowning. 1988. A transient array of parallel microtubules in frog eggs: potential tracks for a cytoplasmic rotation that specifies the dorso-ventral axis. *Dev. Biol.* 128:185–197.

Erickson, H. P., and E. T. O'Brien. 1992. Microtubule dynamic instability and GTP hydrolysis. *Annu. Rev. Biophys. Biomol. Struct.* 21:145–166.

Faruki, S., and E. Karsenti. 1994. Purification of microtubule proteins from *Xenopus* egg extracts: identification of a 230K MAP4-like protein. *Cell Motil. Cytoskeleton.* 28:108–118.

Gard, D. L. 1992. Microtubule organization during maturation of Xenopus oocytes: assembly and rotation of the meiotic spindles. *Dev. Biol.* 151:516–530.

Gard, D. L., and M. W. Kirschner. 1987*a*. Microtubule assembly in cytoplasmic extracts of Xenopus oocytes and eggs. *J. Cell Biol.* 105:2191–2201.

Gard, D. L., and M. W. Kirschner. 1987*b*. A microtubule-associated protein from Xenopus eggs that specifically promotes assembly at the plus-end. *J. Cell Biol.* 105:2203–2215.

Gildersleeve, R. F., A. R. Cross, K. E. Cullen, A. P. Fagen, and R. C. Williams. 1992. Microtubules grow and shorten at intrinsically variable rates. *J. Biol. Chem.* 267:7995–8006.

Gliksman, N., S. F. Parsons, and E. D. Salmon. 1992. Okadaic acid induces interphase to mitotic-like microtubule dynamic instability by inactivating rescue. *J. Cell Biol.* 119:1271–1276.

Gliksman, N. R., R. V. Skibbens, and E. D. Salmon. 1993. How the transition frequencies of microtubule dynamic instability (nucleation, catastrophe, and rescue) regulate microtubule dynamics in interphase and mitosis: analysis using a monte carlo computer simulation. *Mol. Biol. Cell.* 4:1035–1050.

Houlistan, E., and R. Elison. 1991. Patterns of microtubule polymerization relating to cortical rotation in *Xenopus laevis* eggs. *Development (Camb.).* 112:107–117.

Hyman, A. A., S. Salser, D. N. Drechsel, N. Unwin, and T. J. Mitchison. 1992. Role of GTP hydrolysis in microtubule dynamics: information from a slowly hydrolyzable analog, GMPCPP. *Mol. Biol. Cell.* 3:1155–1167.

Kowalski, R. J., and R. C. Williams. 1993. Microtubule-associated protein 2 alters the dynamic properties of microtubule assembly and disassembly. *J. Biol. Chem.* 268:9847–9855.

Lutz, D. A., and S. Inoue. 1986. Techniques for observing living gametes and embryos. *Methods Cell Biol.* 27:89–110.

Mandelkow, E. M., E. Mandelkow, and R. A. Milligan. 1991. Microtubule dynamics and microtubule caps: a time-resolved cryo-electron microscopy study. *J. Cell Biol.* 114:977–991.

McNally, F., and R. D. Vale. 1993. Identification of katanin, an ATPase that severs and disassembles stable microtubules. *Cell.* 75:419–429.

Mitchison, T., and M. Kirschner. 1984. Dynamic instability of microtubule growth. *Nature (Lond.).* 312:237–242.

Mitchison, T., and M. Kirschner. 1988. Cytoskeletal dynamics and nerve growth. *Neuron.* 1:761–772.

Morrisey, J. H. 1981. Silver stain for proteins in polyacrylamide gels: a modified procedure with enhanced sensitivity. *Anal. Biochem.* 117:307–310.

Northrup, S. H., and H. P. Erickson. 1992. Kinetics of protein-protein association explained by Brownian dynamics computer simulation. *Proc. Natl. Acad. Sci. USA.* 89:3338–3342.

O'Brien, E. T., W. A. Voter, and H. P. Erickson. 1987. GTP hydrolysis during microtubule assembly. *Biochemistry.* 26:4148–4156.

O'Brien, E. T., E. D. Salmon, R. A. Walker, and H. P. Erickson. 1990. Effects of magnesium on the dynamic instability of individual microtubules. *Biochemistry.* 29:6648–6656.

Pryer, N. K., R. A. Walker, V. P. Skeen, B. D. Bourns, M. F. Soboeiro, and E. D. Salmon. 1992. Microtubule-associated proteins modulate microtubule dynamic instability *in vitro*: real-time observations using video microscopy. *J. Cell Sci.* 103:965–976.

Salmon, T., R. A. Walker, and N. K. Pryer. 1989. Video-enhanced differential interference contrast light microscopy. *BioTechniques.* 7:624–633.

Sammak, P. J., and G. G. Borisy. 1988. Direct observation of microtubule dynamics in living cells. *Nature (Lond.).* 332:724–726.

Schnapp, B. J. 1986. Viewing single microtubules by video light microscopy. *Methods Enzmol.* 134:561–573.

Schroeder, M. M., and D. L. Gard. 1992. Organization and regulation of cortical microtubules during the first cell cycle of *Xenopus* eggs. *Development (Camb.).* 114:699–709.

Serrano, L., J. Avila, and R. B. Maccioni. 1984. *Biochemistry.* 23:4675–4681.

Schulze, E., and M. Kirschner. 1988. New features of microtubule dynamic instability behavior observed *in vivo*. *Nature (Lond.).* 334:356–359.

Shiina, N. T., Y. Gotoh, and E. Nishida. 1992*a*. A novel homo-oligomeric protein responsible for an MPF-dependent microtubule-severing activity. *EMBO (Eur. Mol. Biol. Organ.) J.* 11:4723–4731.

Shiina, N. T., T. Moriguchi, K. Ohta, Y. Gotoh, and E. Nishida. 1992*b*. Regulation of a major microtubule-associated protein by MPF and MAP kinase. *EMBO (Eur. Mol. Biol. Organ.) J.* 11:3977–3984.

Sheldon, E., and P. Wadsworth. 1993. Observation and quantification of individual microtubule behavior in vivo: microtubule dynamics are cell-type specific. *J. Cell Biol.* 120:935–945.

Simon, J. R., S. F. Parsons, and E. D. Salmon. 1992. Buffer conditions and non-tubulin factors critically affect the microtubule dynamic instability of sea urchin egg tubulin. *Cell Motil. Cytoskeleton.* 21:1–14.

Stewart-Savage, J., and R. D. Grey. 1982. The temporal and spatial relationships between cortical contraction, sperm tail formation, and pronuclear migration in fertilized *Xenopus* eggs. *Wilhelm Roux's Arch. Dev. Biol.* 191:241–245.

Stewart, R. J., K. W. Farrell, and L. Wilson. 1990. Role of GTP hydrolysis in microtubule polymerization: evidence for a coupled hydrolysis mechanism. *Biochemistry.* 29:6489–6498.

Tanaka, E. M., and M. W. Kirschner. 1991. Microtubule behavior in the growth cones of living neurons during axon elongation. *J. Cell Biol.* 115:345–363.

Toso, R. J., M. A. Jordan, K. W. Farrell, B. Matsumoto, and L. Wilson. 1993. Kinetic stabilization of microtubule dynamic instability in vitro by vinblastine. *Biochemistry.* 32:1285–1293.

Vale, R. D. 1991. Severing of stable microtubules by a mitotically activated protein in *Xenopus* egg extracts. *Cell.* 64:827–839.

Verde, F., M. Dogterom, E. Stelzer, E. Karsenti, and S. Leibler. 1992. Control of microtubule dynamics and length by cyclin A- and cyclin B-dependent kinases in *Xenopus* egg extracts. *J. Cell Biol.* 118:1097–1108.

Voter, W. A., and H. P. Erickson. 1984. The kinetics of microtubule assembly. *J. Biol. Chem.* 259:10430–10438.

Walker, R. A., E. T. O'Brien, N. K. Pryer, M. F. Soboeiro, W. A. Voter, H. P. Erickson, and E. D. Salmon. 1988. Dynamic instability of individual, MAP-free microtubules analyzed by video light microscopy: rate constants and transition frequencies. *J. Cell Biol.* 107:1437–1448.

Walker, R. A., N. K. Pryer, and E. D. Salmon. 1991. Dilution of individual microtubules observed in real time *in vitro*: evidence that cap size is small and independent of elongation rate. *J. Cell Biol.* 114:73–81.